Environmental Technology & Innovation 40 (2025) 104654

Contents lists available at ScienceDirect

Environmental Technology & Innovation

journal homepage: www.elsevier.com/locate/eti

Comparative analysis of indoor and outdoor airborne microplastics in a school in Vilnius, Lithuania

Steigvilė Byčenkienė [a,*], Ieva Uogintė [a], Lina Davulienė [a], Sergej Šemčuk [a], Mehri Davtalab [a], Vadimas Dudoitis [a], Simonas Kecorius [a,b,c], Mario Lovrić [d,e]

[a] Center for Physical Sciences and Technology (FTMC), Saulėtekio av. 3, Vilnius LT-10257 Lithuania
[b] Institute of Epidemiology, Helmholtz Zentrum München - German Research Center for Environmental Health, Neuherberg, Germany
[c] Environmental Science Center, University of Augsburg, Augsburg, Germany
[d] The Lisbon Council, Brussels 1040, Belgium
[e] Institute for Anthropological Research, Zagreb 10000, Croatia

ARTICLE INFO

Keywords:
Airborne microplastic
Indoor exposure
Source apportionment
Inhalation risk
Northern Europe

ABSTRACT

Airborne microplastics (MPs) poses a potential health risk, particularly in sensitive microenvironments such as schools, where children are subject to prolonged exposure durations. This study investigates airborne MPs indoors and outdoors at an urban school from December 2023 to April 2024, quantifying concentrations and characterizing morphology, polymer composition, and sources. Comparative analysis revealed distinct indoor-outdoor differences in chemical composition, source attribution, and associated risks. Indoors were dominated by polyester (33.0 %) and acrylates (31.1 %), while outdoor were primarily composed of polyethylene (48.6 %) and polypropylene (7.7 %). Source apportionment modeling identified textiles (31.0 %) and packaging (30.6 %) as the primary indoor contributors, whereas outdoor MPs were largely linked to packaging (46.3 %) and transport-related emissions (28.1 %). Morphologically, fibers predominted indoors (66 %), reflecting synthetic textile shedding, whereas fragments dominated outdoors reaching (up to 94 %). Statistically significant correlations between indoor and outdoor MPs profiles (Mantel $r \geq 0.5$, $p \leq 0.001$) underscored the influence of air exchange and infiltration processes. We present the first study in Northern Europe to characterize airborne microplastics in a school located near a high-traffic road, analyzing both outdoor and indoor air to determine particle morphology, chemical composition, dispersion patterns, and likely sources.

1. Introduction

Indoor air quality (IAQ) in schools is a critical factor influencing not only children's health and well-being but also their academic performance (McCormack et al., 2018). Literature suggests that children spend 800–900 h per year in schools settings (Education at a Glance, 2023). Given this substantial indoor time, understanding and mitigating airborne microplastics (MPs) exposure is crucial for protecting health (Liu and Zheng, 2025). Schools are increasingly recognized as critical microenvironments where, due to developing physiology and longer indoor occupancy, children may encounter complex mixtures of airborne pollutants. Unlike better-known indoor air pollutants such as particulate matter (PM), airborne MPs are novel and an emerging concern. Their small size and diverse

* Corresponding author.
E-mail address: steigvile.bycenkiene@ftmc.lt (S. Byčenkienė).

https://doi.org/10.1016/j.eti.2025.104654
Received 28 August 2025; Received in revised form 5 November 2025; Accepted 23 November 2025
Available online 25 November 2025

physicochemical properties enable multiple exposure pathways, including inhalation, ingestion, and dermal contact, raising important questions about potential health implications (O'Leary, 2024). MPs and PM are distinct yet interconnected pollutants in indoor air, particularly within school environments. While differing in origin, composition, and morphology, both can coexist in the same air matrix, potentially interacting and contributing to cumulative exposure risks for children. Furthermore, both can act as vectors (Arvaniti et al., 2022; Pomata et al., 2024) or reservoirs for chemicals and microorganisms, transporting them deeply into the respiratory tract upon inhalation. Once inhaled, these particles can deposit throughout the airways and may trigger inflammation and oxidative stress. Ingestion and dermal exposure may also produce systemic effects that require further investigation (Luo et al., 2025). Children's higher breathing rates relative to body further increase susceptibility to inhaled contaminants. MPs can be inhaled and can accumulate in the respiratory tract and lungs (Jenner et al., 2022), leading to lung inflammation (Zarus et al., 2021), contribute to cardiovascular disease (Marfella et al., 2024) and potentially lead to other adverse health outcomeses (Nihart et al., 2025). This raises concerns regarding the association between the MPs intake and potential health risks in indoor residential environments.

Recent studies demonstrate that breathable microplastics (smaller than 5 μm) overlap the regulated particulate size ranges, underscoring the physical nexus between MPs and PM (Maurizi et al., 2024). Similarly, Morioka et al., (2024)) reported substantial quantities of airborne MPs within 0.43–11 μm range, indicating that a significant fraction falls within the PM_{10} category. Nandi et al. (2024) further identified MPs ranging from less than 1 μm to 40 μm indoors and outdoors (Bhat, 2024a). It's important to note that the shape of the MP particles also plays a role. Fibrous MPs may have considerable length but small aerodynamic diameter, so they can be classified as PM based on their diameter even if their length exceeds the PM size range. This adds another layer of complexity to the relationship between MP and PM (Maurizi et al., 2024). Mass-based estimates suggest that MPs typically constitute a small but non-negligible fraction of PM. For instance, studies reported that MPs accounted for approximately 0.1–0.4 % of PM_{10} and 0.01–0.3 % of $PM_{2.5}$ mass concentrations in urban and suburban environments in China (Chen et al., 2020; Liu et al., 2019a). Studies conducted in European cities have yielded comparable results, Allen et al. (2019) (Allen et al., 2019a) estimated that MPs may represent up to 1.5 % of total atmospheric PM, while (Materić et al., 2020) detected MPs in $PM_{2.5}$ samples from remote and urban sites in the Netherlands, with mass contributions likely below 0.01 %. Although these values represent a minor fraction of total PM mass, potentially high number concentrations, especially in fibrous form, and the capacity of MPs to carry additives or adsorbed pollutants elevate their relevance in air quality and health assessments. Cross-study comparisons should be interpreted with care, as differences in size thresholds, sampling approaches and analytical confirmation may influence results.

Research on MPs in school air is still in its early stages, yet initial findings raise concerns about children's exposure. MPs can infiltrate classrooms through multiple pathways, including tracked-in dust, airborne deposition, and the fragmentation from indoor materials (Abbasi et al., 2022). Routine activities such as cleaning or ventilation can resuspend settled particles, increasing the inhalation potential for students and staff. Abbasi et al., (2022) (Abbasi et al., 2022) reported substantial MP loads, predominantly fibers, in settled classroom dust, highlighting schools as important indoor exposure environments. Complementary findings by (Nandi et al., 2024) characterized MPs in both indoor and outdoor air across seasons in a school setting. Their results showed higher indoor MP levels in winter and summer, while outdoor deposition rates were significantly greater in $PM_{2.5}$ fractions compared to PM_{10}, particularly in winter. Indoors, deposition rates were lower than outdoors, but still substantial, increasing from 8.3×10^4 particles/m^2/day (post-monsoon) to 1.03×10^5 particles/m^2/day (winter). In both settings, fibers dominated MP morphology. These findings underscore the need assessi and mitigate MP exposure in schools, particularly given the vulnerability of children.

The detection of MPs in human tissues organs, as reported in some studies (Sharma et al., 2024; Zhu et al., 2024; Zhang et al., 2025; Zipeng et al., 2025), is a significant finding. Although the direct health consequences of MP accumulation remain under investigation, growing evidence suggests potential biological effects, including inflammation and oxidative stress in various cell types and tissues (Chakraborty et al., 2024; K C et al., 2023; Kumar et al., 2025). Emerging studies also suggest potential disruption of hormonal, immune, and reproductive functions (Wang et al., 2024; Pathak, 2025). Nevertheless, interdisciplinary studies are needed to clarify mechanisms of interaction (e.g., particle size/shape, polymer and additive profiles), dose–response relationships, and the long-term health implications of exposure across diverse environmental contexts (Cui et al., 2025).

The observed seasonal increase in indoor MP concentrations is attributed to reduced ventilation during winter, when windows and doors are typically remain closed, leading to the accumulation of indoor sources. This period also coincides with greater use of synthetic textiles and packaging, which may elevate indoor MP levels. Notably, a predominance of smaller MPs (1–50 μm) was reported in classroom air, highlighting the potential for inhalation exposure among students and staff. A recent review by Kek et al., (2024) (Kek et al., 2024) provides a broader view of airborne MPS in indoor environments, including schools, and emphasizes the health risks particularly from particles from < 1 μm to several hundred micrometers. Complementing this, (Zhai et al., 2023)characterized and quantified airborne MPs across indoor settings, reporting concentrations ranging from 0.27 to 4.99 particles/m^3 . Despite these advances, size-resolved, standardized measurements in child-centric environments remains limited, reinforcing the need for expanded datasets. Beyond basic occurrence and composition, studies seldom integrate multiple particle attributes (polymer, morphology, color, size) into a single, transparent source apportionment and rarely evaluate robustness of the resulting inferences. Accordingly, this study pursued two objectives: (i) to quantify airborne MPs in indoor and outdoor areas of a school and examine the relationship between indoor and outdoor MP characteristics; and (ii) to characterize MP attributes, including size distribution, color, and predominant polymer types. This work advances the field by integrating a time-resolved indoor-outdoor dataset with a robustness-tested, multi-attribute source apportionment (polymer, morphology, color, size), and by introducing a unitless, comparative Inhalation Hazard-Weighted Abundance Index (IHWAI) calculated by REACH/CLP heuristics and morphology to rank samples by hazard-weighted composition. To our knowledge, this combination has not previously been reported for airborne microplastics in school environments. Additionally, we investigated rubber sources to identify and distinguish black MPs originating from rubber-based materials such as tires, footwear, and industrial components. This knowledge is essential for identifying key factors

influencing MP presence, distribution, and properties, ultimately informing the development of effective mitigation strategies to reduce exposure and safeguard children's health.

2. Methods

2.1. Study area, sampling and preparation

This study, which is part of a broader undertaking in the Horizon Europe EDIAQI project (*EDIAQI Project - Evidence Driven Indoor Air Quality Improvement)* which monitors indoor air quality across Europe, was conducted in an indoor environment of a school located in downtown Vilnius, Lithuania. The region experiences a humid continental climate with warm summers and cold, snowy winters. The school is near traffic, with roads approximately 60 m to the west, 20 m to the north, and 10 m the south of the buiding. Sampling was conducted from December 2023 to April 2024, encompassing the winter and early spring seasons. During each sampling period, three individual samples were collected and combined into a single composite sample, resulting in a total of 11 indoor and 15 outdoor composite samples. This window was selected to capture conditions typical of the heating season, when indoor ventilation is reduced and resuspension/textile shedding may be enhanced in occupied classrooms.

Passive indoor air sampling was conducted in a second-floor classroom using glass fiber filters mounted ~ 1.6 m above the floor level and positioned away from doors to minimize disturbance from occupant movement. This placement corresponds to the typical human breathing zone (~1.5 m), in accordance with established indoor air quality monitoring guidelines, ensuring that the measurements accurately reflect occupant exposure. Outdoor sampling was performed at a monitoring container adjusted to the school, with the inlet set at ~3 m above ground level, consistent with ambient air quality monitoring practice representative ambient conditions (EPA, 2025). This method was chosen as it offers several advantages in the school setting, it operates silently and non-intrusively during the learning process, is easy to deploy, cost-effective, and allows integration of exposure assessment. Nevertheless, future studies should complement passive approaches with active air sampling techniques (e.g., cascade impactors, pumps with size-selective inlets) to provide a more comprehensive characterization. It should be noted that passive deposition primarily reflects the settled fraction of airborne particles and therefore may underrepresent the suspended fine fraction (<10 μm) most relevant for direct inhalation exposure.

Indoors, temperature remained stable throughout the campaign (mean ~26.9 ± 0.4 °C), reflecting regulated heating conditions, while RH was consistently low (mean ~21.4 ± 3.4 %), particularly during cold months. Elevated CO_2 concentrations (mean ~790 ± 359 ppm, up to 1034 ppm in January) indicated limited ventilation and high occupancy, conditions that favor the accumulation of suspended particles and MPs and secondary fiber resuspension. Mean indoor $PM_{2.5}$ levels (4.3 ± 2.5 μg m^{-3}) were moderate, with episodic increases coinciding with elevated CO_2 and MPs deposition, suggesting reduced air exchange efficiency during cold periods. By contrast, outdoor temperature displayed strong seasonal variability (mean ~3.7 ± 3.6 °C, range –9–15 °C), while relative humidity remained high (mean ~71 ± 11 %). Outdoor $PM_{2.5}$ concentrations (15.8 ± 10.2 μg m^{-3}) were typically higher than indoors, particularly in winter, consistent with regional heating emissions and atmospheric stability that limit dispersion. CO_2 levels outdoors (mean ~453 ± 18 ppm) were near background values and showed minimal variation. The lowest outdoor temperatures and highest $PM_{2.5}$ values were recorded in January–February, reflecting winter inversion conditions conducive to pollutant accumulation. Overall, these contrasts demonstrate that the indoor environment is thermally stable but poorly ventilated, leading to enhanced retention and resuspension of microplastics, while outdoor air is more dynamic, dominated by temperature-driven dispersion and seasonal emission cycles. The simultaneous peaks in indoor CO_2, $PM_{2.5}$, and MP concentrations highlight the influence of human activity and ventilation on indoor particle dynamics, whereas outdoor MP levels were more closely linked to traffic-related sources, resuspended road dust, and meteorological variability.

The indoor sampling device consists of a Glass Petri dish with filter paper. To ensure data reliability, two parallel experiments were conducted at each sampling point. The sampler was positioned 1.20 m above the ground, corresponding to breathing height, and fully exposed to the atmosphere during sampling.The sampling device for outdoor samples remained the same, with the only variation being that it was shielded from precipitation while still allowing for air flow. Upon arrival at the laboratory, particles collected on glass fiber filters were carefully transferred to pre-cleaned glass beakers containing distilled water. To remove organic matter, each sample was treated with a 30 % hydrogen peroxide (H_2O_2) solution (Sigma-Aldrich, Germany) and left to react for 24 h. Afterward, a saturated zinc chloride ($ZnCl_2$) solution, with a density ranging from 1.6 to 1.8 g/cm^3 , was used to separate MPs particles from other particulates. Samples were transferred to a separating funnel containing the $ZnCl_2$ solution and left for several hours to allow for stratification. During this flotation process, MPs, being less dense, rose to the surface, while denser non-plastic materials settled at the bottom. The supernatant containing the MPs was then filtered through glass fiber filters ("Branchia" filters, 50 mm diameter, 1.6 μm pore size). The filters were subsequently dried at 60 °C for 24 h. After drying, the filters were examined under a digital optical microscope equipped with a 200 × objective lens for preliminary identification and characterization of MP particles. During the analysis of microplastic particles the blank glass fiber filter were exposed to laboratory air.

Each MP particle was categorized according to its size, shape, and color. The longest dimension of each MP was measured using the *Motic Images Plus 3.0* software. Particles were then grouped into six size classes: < 50 μm, 50–100 μm, 100–250 μm, 250–500 μm, 500–1000 μm, and > 1000 μm. Morphological classification distinguished particles as either fibers or fragments. Color was recorded visually under microscope, with particles categorized as black, brown, white, blue, red, yellow, or other discernible colors. To determine the polymer composition, selected particles were transferred onto Al_2O_3 filters and analyzed using micro-Fourier transform infrared (μ-FTIR) spectroscopy (LUMOS II, Bruker, Germany) in the 4000–1200 cm^{-1} spectral range. The size detection limit of the μ-FTIR analysis was > 5 μm, and thus only MPs larger than this threshold were identified. Each measurement consisted of four scans,

and the resulting spectra were compared to the instrument's internal reference library. A particle was identified as a MP if the spectral match with a known polymer exceeded 70 % similarity. The identified polimers included acrylates (ACR), alkyd (ALK), nitrile butadiene rubber (NBR), polyamide (PA), polyimide (PI), polyester (PES), polyethylene (PE), polyisoprene (PIR), polypropylene (PP), polystyrene (PS), polytetrafluoroethylene (PTFE), polyurethane (PU), polyvinyl chloride (PVC), and rubber (see Table 1 for full details).

2.2. Quality assurance and quality control

Strict contamination control protocols were implemented throughout the sampling and analytical procedures to ensure data accuracy and minimize the risk of airborne MPs contamination. Following each 24-hour sampling period, Petri dishes were immediately sealed and covered with aluminum foil to prevent exposure to airborne particles. All extraction steps were performed within a laminar-flow hood to maintain a particle-free working environment. Prior to use, all glassware was thoroughly rinsed with Milli-Q water to eliminate potential residual contaminants. To minimize the introduction of synthetic fibers, laboratory personnel wore 100 % cotton lab coats and sterile nitrile gloves during all stages of sample handling and analysis. Additionally, laboratory blanks were processed in parallel with environmental samples to monitor and account for any potential background contamination. Collectively, these measures ensured the reliability, consistency, and validity of the analytical results. Quality control procedures during the processing of microplastic particles from air samples followed the guidelines outlined in the literature (Dewika et al., 2025; Ferraz et al., 2024).

2.3. Microplastic source apportionment model

To estimate the relative contribution of different indoor sources to airborne MPs, a semi-quantitative source attribution model was developed based on particle composition and physical characteristics. The approach aimed to differentiate MPs originating from major indoor categories: Textiles, Packaging, Flooring, and Outdoors inputs (outdoor specific subclasses, i.e., tire wear). The model utilized measured parameters including particle polymer type, shape (fibers or fragments), color, and size distribution. These features were selected due to their established associations with specific material types and environmental behaviors. For example, PES and PA are typically linked to textile shedding (Dris et al., 2016a), (Vianello et al., 2019a), while PP and PE are widely used in packaging materials. Polymers such as PVC, rubber compounds, and PS were linked to flooring, insulation, and building materials (Wright and Kelly, 2017). Black and red particles, which are frequently associated with tire wear and other outdoor sources, were used as indicators of outdoor MPs contributions (Zhang et al., 2020; Allen et al., 2019b). Each feature was assigned a set of relative weightings (ranging from 0 to 1) indicating its likelihood of originating from each of the four source categories. These weightings reflected the probability that a given feature originated from a particular source and were based on empirical data and material usage patterns reported in previous studies (Wright and Kelly, 2017), (Liu et al., 2019b). For each sampling date, the measured relative abundance of each feature was multiplied by its corresponding source-specific weights. The resulting values were aggregated per source category to produce a raw source contribution score. These scores were subsequently normalized so that the total contribution across all sources equaled 100 %, yielding an estimated percentage contribution of each source category for every sample (Table 1).

This approach enabled the identification of both background emissions (e.g., persistent textile shedding) and episodic inputs, such

Table 1
Normalized feature–source weight matrix by material, morphology, color, and size.

Feature	Textiles	Packaging	Flooring	Outdoors
Polyester	1.0	0.1	0.0	0.0
Polyamide	0.1	0.3	0.3	0.3
Polypropylene	0.2	1.0	0.2	0.1
Polyimide	0.1	0.2	0.3	0.4
Polyethylene	0.1	1.0	0.1	0.2
Polyvinylchloride	0.0	0.2	1.0	0.2
Polystyrene	0.0	0.5	0.3	0.2
Rubbers	0.0	0.1	0.4	1.0
Polyisoprene	0.0	0.1	0.3	1.0
Nitrile butadiene rubber	0.0	0.2	0.5	0.3
Acrylates	0.3	0.5	0.2	0.0
Fibers	1.0	0.0	0.0	0.0
Fragments	0.0	1.0	0.3	0.3
Black*	0.0	0.2	0.2	1.0
Red	0.1	0.3	0.2	0.4
Blue	0.3	0.4	0.2	0.1
Green	0.2	0.3	0.3	0.2
< 50 μm	0.6	0.3	0.2	0.3
50–100 μm	0.5	0.4	0.2	0.3
100–250 μm	0.4	0.5	0.3	0.2
250–500 μm	0.3	0.5	0.4	0.2
500–1000 μm	0.2	0.5	0.5	0.3
> 1000 μm	0.1	0.4	0.6	0.4

* Black for flooring and tires

as packaging- or flooring-related fragments, as well as periods potentially influenced by outdoor infiltration. The source apportionment results are semi-quantitative, representing indicative trends rather than precise quantitative estimates, as the weighting matrix was derived from literature-based proxies and the authors' expert judgment. Therefore, the results should be interpreted as comparative rather than absolute values. Certain features (e.g., color categories or larger size bins) may overlap across multiple sources, potentially leading to misclassification. Although sensitivity analysis indicated that the main findings (e.g., textiles identified as the dominant indoor source) are robust to reasonable variations in the weighting matrix, the outcomes should nevertheless be regarded as indicative trends rather than exact quantitative estimates.

2.4. Inhalation hazard-weighted abundance index (IHWAI)

To compare samples on a common scale, a unitless, comparative index that weights the relative abundance of observed features by REACH/CLP-informed hazard heuristics (monomer/additive profiles) and by morphology relevance for inhalation was calculated. The IHWAI is a hazard-weighted abundance metric, not a quantitative risk assessment. It does not integrate inhaled dose, deposition fractions by size, or dose–response. Additive leaching and degradation kinetics were not modeled. Each polymer type identified was assigned a toxicity weighting on a scale from 0 (low concern) to 1 (high concern), based on the regulation on the registration, evaluation, authorization and restriction of chemicals (REACH) databases by EU law to protect human health and the environment from the risks that can be posed by chemicals.

For each sample, the index was calculated as:

$$\mathrm{IHWAI} = \sum_{p} \mathrm{ApWp} + (\mathrm{AfibersWfibers} + \mathrm{AfragmentsWfragments}) \tag{1}$$

where:

A_p - the row-normalized polymer composition among identified polymers W_p - $\in[0,1]$ are heuristic hazard weightings

A_{fibers}, $A_{fragments}$ are morphology fractions (fibers assigned higher weighting than fragments)

PVC received the highest toxicity weighting (1.0)A due to its chlorine content, the presence of phthalate plasticizers, and its potential to release hazardous combustion by-products. Rubber-based polymers, including PIR and nitrile rubber were similarly assigned high scores (0.9) due to their known content of carcinogenic polycyclic aromatic hydrocarbons (PAHs), heavy metals, and vulcanization agents. Moderate-risk polymers such as ACR and PS were assigned intermediate weightings (0.7), reflecting their potential to release harmful monomers and additives. In contrast, relatively inert polymers such as PE and PP were assigned lower toxicity scores (0.3–0.4) consistent with their widespread use and lower chemical reactivity. In addition to polymer identity, particle morphology was incorporated into the inhalation risk index by assigning higher risk values to fibrous particles (weight = 0.9) (Vianello et al., 2019b), which have a greater propensity for deep lung deposition, compared to fragmented particles (weight = 0.5). The final inhalation risk score for each sample was calculated as the sum of the abundance of MP particles, each weighted by their respective polymer toxicity and morphology scores. This value was then normalized to produce a unitless inhalation risk index, allowing for comparative assessment across indoor and outdoor environments.

2.5. Statistical approach

The Mantel test using the R programming language, originally developed for assessing the correlation between two distance or

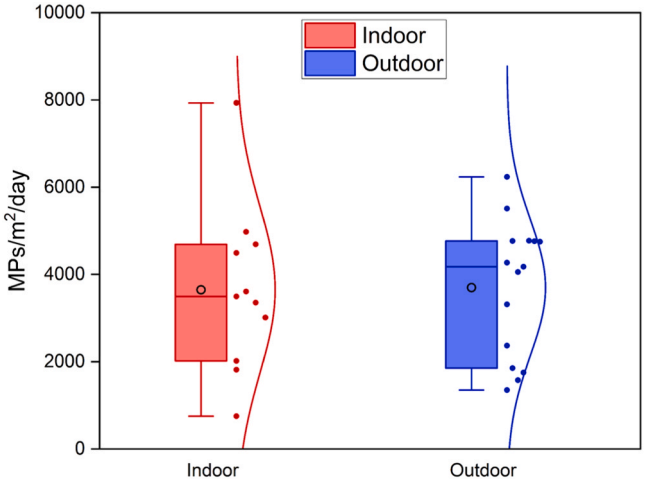

Fig. 1. The box and whiskers plot of indoor and outdoor MPs count. The medians and means (dot line) are indicated with horizontal lines dividing each box, and the whiskers are set to the lowest and the highest value when they are not outliers (the values above or below 1.5 × IQR, indicated as black crosses).

similarity matrices, was applied here to quantify the statistical relationship between indoor and outdoor MPs profiles based on their polymer composition, morphology, and environmental variables. The statistical analyses and graphical visualizations were performed using OriginPro (OriginLab Corporation, Northampton, MA, USA), a licensed data analysis and graphing software widely used in environmental and aerosol research. The chemical composition of microplastic particles was determined with a LUMOS II micro-spectrometer and processed with the OPUS 9.1 software. The spectra and physical properties of the particles detected on the filter were determined by processing them with the artificial intelligence-based OPUS plugin MP-ID. The MP-ID software automatically analyzes whole FT-IR images of microplastic samples and yields comprehensive statistics of all particles present on the filter, classifying them by number, identity, and size.

3. Results and discussion

3.1. Total MPs abundance

Statistical analysis of MPs concentrations in indoor and outdoor environments revealed significant differences in their distribution and variability. On average, indoor MP levels were slightly higher than those observed outdoors levels. The mean and median concentrations indoors were 4127 and 3851 MPs/m^2/day, respectively, compared to 3533 and 3313 MPs/m^2/day outdoors (Fig. 1). Outdoor MP levels exhibited a relatively narrower range (approximately 1352–6236 MPs/m^2/day), whereas indoor concentrations spanned a substantially broader range (754–7933 MPs/m^2/day). This disparity was further reflected in the standard deviations, which were $\sigma = 1731$ for outdoor samples and $\sigma = 2556$ for indoor samples. These findings underscore the greater variability and dynamic nature of MP presence in indoor environments, likely influenced by localized sources, occupant activities, and building-specific factors. In contrast, the more constrained variability outdoors may reflect more uniform environmental conditions and enhanced atmospheric dispersion. The lowest indoor MP concentration was observed during the period of December 11–25, 2023 (753 MP/m^2/day). This period coincided with the winter holidays, characterized by reduced human occupancy and minimal indoor activity, which likely contributing to the lower MP levels. In contrast, the highest concentration was observed during March 4–11, 2024, reaching 7933 MP/m^2/day, suggesting a substantial short-term increase of MPs load, potentially associated with intensive indoor activity, particle resuspension, or external intrusion (e.g., open windows or cleaning events). These findings support the hypothesis of seasonal or occupancy-driven fluctuations in indoor microplastic pollution, highlighting the importance of temporal factors in exposure assessments.

The narrower range and lower standard deviation of outdoor MPs concentrations suggest that atmospheric dispersion mechanisms, such as wind and precipitation, play a key role in regulating ambient MP levels (Wright et al., 2020). In contrast, the greater variability observed indoors reflects the influence of localized sources, including human occupancy, ventilation dynamics, and material shedding from textiles and other plastic-containing item (Kek et al., 2024; Zhai et al., 2023; "EDIAQI Project - Evidence driven indoor air quality improvement, 2025; Dewika et al., 2025; Ferraz et al., 2024; Dris et al., 2016a; Vianello et al., 2019a; Wright and Kelly, 2017; Zhang et al., 2020). The outdoor MPs concentrations observed in this study largely exceeded most values reported in previous studies across various urban environments. For instance, reported urban MP deposition rates include 10 ± 8 MP/m^2/day (5 – 5000 μm) in Gdynia, Poland (Szewc et al., 2021), 0.4 MP/m^2/day Kusatsu, Japan, 4.0 MP/m^2/day Da Nang, Vietnam, 12.5 MP/m^2/day Kathmandu and Nepal (Yukioka et al., 2020), and 114 ± 40 MP/m^2/day Guangzhou, China (Huang et al., 2021). Even in densely populated urban centers such as Central London, with reported deposition rates ranging from 575 to 1008 MPs/m^2/day (mean: 771 ± 167 MPs/m^2/day for particles >5 μm) (Wright et al., 2020), and Christchurch, New Zealand (80–1018 MP/m^2/day) (Knobloch et al., 2021), the concentrations were lower than those we observed in this study. Among the few studies reporting comparably high deposition rates, Paris, France stands out, with values ranging from 1586 to 11,130 MPs/m^2/day (for particles >50 μm), making it one of the closest in magnitude to our findings (Niu et al., 2024).

These findings suggest that metropolitan environments characterized by high traffic density and diverse emission sources can exhibit substantially elevated MPs deposition rates. The consistently high outdoor MPs levels observed in this study are likely influenced by the sampling location proximity to multiple roads, leading to increased vehicular emissions and the resuspension of road-derived MPs. While outdoor MPs pollution has been relatively well studied, indoor MP concentrations, particularly in school environments, remain underexplored. Al-Hussayni et al. (2023) reported indoor MP concentrations of 4743 ± 427 MPs/m^2/day in kindergartens and 2238 ± 309 MPs/m^2/day in schools in Iraq, indicating substantial exposure levels (Al-Hussayni et al., 2023). In contrast, Bhat (2024) (Bhat, 2024a) reported lower concentrations in educational settings, ranging from 180 to 240 MPs/m^2/day. These variations underscore the influence of local environmental conditions, building characteristics, and occupancy patterns on indoor MP pollution. Importantly, cross-study comparisons are only valid when particle size ranges are explicitly matched.

3.1.1. Morphological properties

3.1.1.1. Color

3.1.1.1.1. Indoor. Black MP particles were the most prevalent, comprising an average of 53 % of all detected particles. Their consistent dominance suggests a strong contribution from tire wear, soot, degraded synthetic rubber, and dark-colored textiles. The peak proportion of 62 % was observed during December 11–25, 2023 (Fig. 2). This finding aligns with previous studies reporting the predominance of black and dark-colored MPs in both indoor and outdoor environments (Abbasi et al., 2022); (Chenappan et al., 2024). Blue MPs represented the second most common color category, accounting for an average of 26 % of total particles, with a peak of

33 % recorded between February 26 and March 4, 2024. This observation is consistent with other studies where blue MPs are frequently reported as dominant or co-dominant in indoor air samples (Chenappan et al., 2024). In contrast, white MPs particles remained relatively low throughout the sampling period, comprising an average of 6 %, with a maximum of 11 % detected February 5–12, 2024.

This observation aligned with findings from other studies (Nandi et al., 2024), where transparent or white particles, commonly linked with plastics like PP and PE are not the most abundant color. Yellow MPs exhibited fluctuating abundances, generally remaining at low levels (average 4 %), with a peak of 9 % observed between February 12–19, 2024. Brown MPs showed a similar pattern, also peaked during this period, suggesting a potencial common source or influencing factor for these colors. Red and green MPs constituted smaller proportions (averaging 5 % and 1 %, respectively), with peaks observed around December 25–January 8, 2024 (6 % red) and December 11–25, 2023 (4 % green), respectively. Color-based correlation analysis revealed a weak positive association between total MP concentrations and the abundance of blue particles ($r = 0.23$), suggesting that higher overall MP levels may be partially driven by sources contributing blue fibers or fragments. In contrast, black particles exhibited a slight negative correlation ($r = –0.18$) with total MP levels, indicating a potential decoupling from peak pollution events and possibly reflecting more stable or persistent sources.

3.1.1.2. Outdoor. Analysis of color distribution revealed that black and white MPs were the most prevalent in the outdoor environment, consistently accounting for the largest proportions of total particles (Fig. 3). Black MPs emerged as the dominant category, comprising over 50 % of total MPs on multiple sampling dates, such as on December 18, 2023 (61 %) – January 1, 2023 (62 %), and February 1, 2024 (52.58 %). This consistent dominance suggests a strong contribution from common outdoor sources such as tire wear, degraded rubber materials, and industrial plastics, which frequently contain black pigments. The prevalence of black MPs in outdoor air underscores their role as a key component of urban microplastic pollution and a potential tracer for non-exhaust traffic emissions.

White MPs were also notable, though present in smaller proportions (approximately 10 %) compared to black MPs. They accounted for substantial shares of total MPs on specific dates, including 12 % on January 1, 2024, and 13 % on February 6, 2024. White MPs are typically derived from a variety of consumer products, such as packaging materials, plastic bottles, and plastic films. Their presence in the outdoor environment reflects the considerable contribution of everyday plastic waste, particularly from packaging debris and discarded plastic items.

3.1.2. Size and shape

3.1.2.1. Indoor. In terms of size distribution, the MPs were primarily dominated by medium-sized fractions. The 100–250 μm size range was the most abundant, contributing on average 32 % of the total particles (Fig. 4). This fraction reached its highest proportion of 57 % during February 26–March 4, 2024. Other notable fractions included the 250–500 μm range (25 %) and the 500–1000 μm range (19 %), both of which exhibited relatively stable proportions throughout the dataset. Notably, both fractions experienced moderate peaks, with the 250–500 μm range reaching 30 % during February 5–12, 2024, and again during March 25–April 1, 2024. Similarly, the 500–1000 μm range peaked at 28 % during February 19–26, 2024. The consistent presence of larger MPs fractions (250–1000 μm) indicated a continuous input of these sizes into the indoor environment. The largest observed MPs (>1000 μm) showed substantial fluctuations in their proportions, particularly on January 28–February 5, 2024 (6 %), and April 1, 2024 (16 %). This variability may be attributed to episodic changes in the sources of coarse plastic debris, such as the degradation or disturbance of larger plastic items through human activity. Although these larger MPs are less likely to remain airborne for extended periods, they may still pose a risk when resuspended.

The smallest MPs fraction (<50 μm) constituted only ~1 % of the total MPs on average, indicating that fine MPs were present but

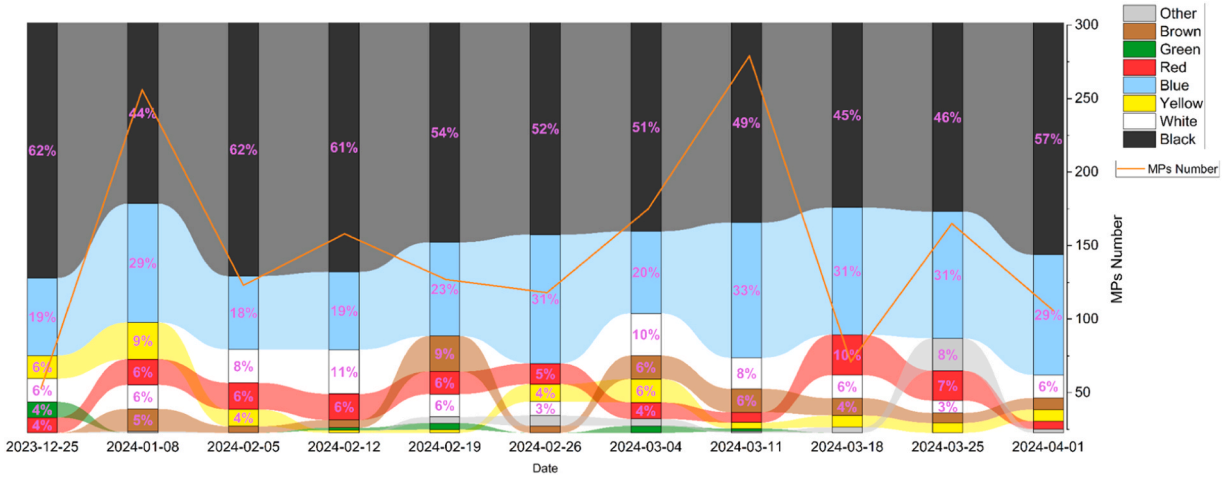

Fig. 2. Color distribution of MPs in the indoor environment.

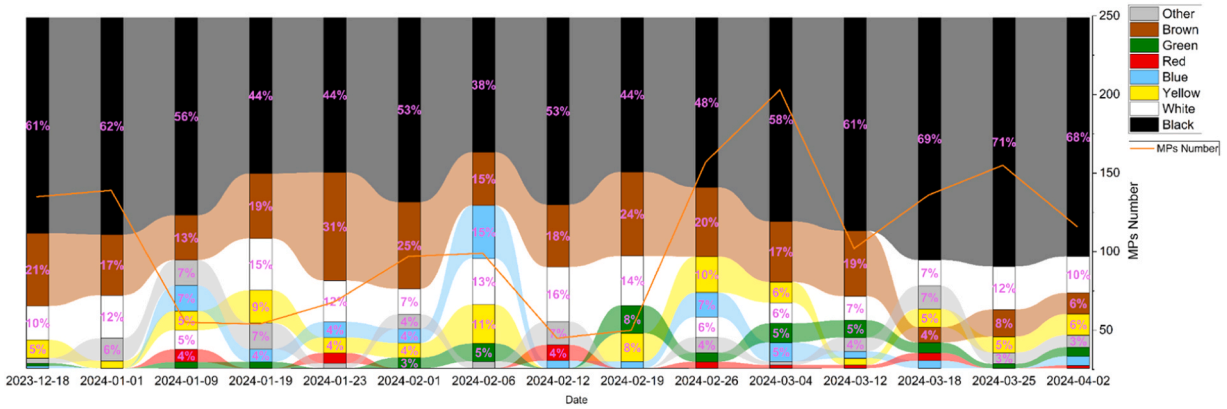

Fig. 3. Color distribution of MPs in the outdoor environment.

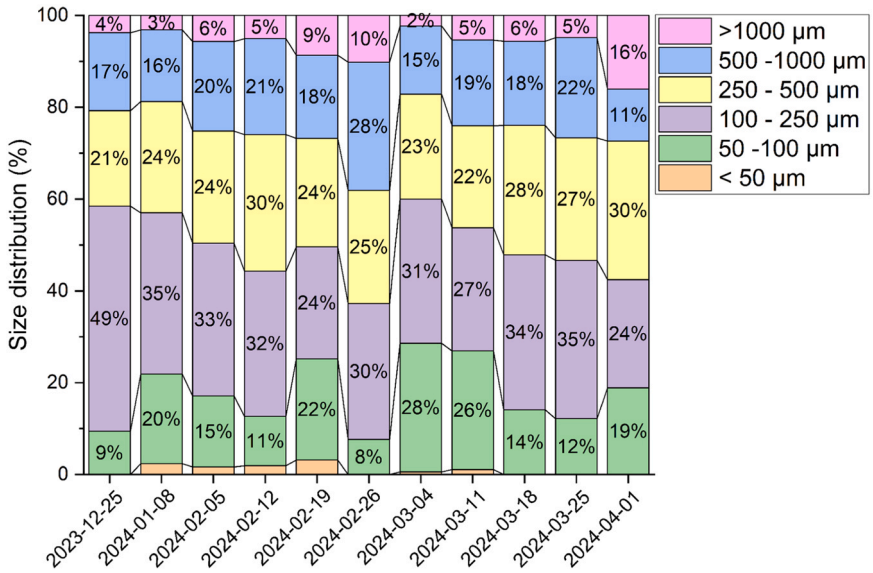

Fig. 4. Size distribution of microplastics collected in indoor air. The data are categorized into five size bins: < 50 μm, 50–100 μm, 100–250 μm, 250–500 μm, and 500–1000 μm. The y–axis represents the percentage of total MPs falling within each size category.

considerably less abundant than larger fractions. This may be attributed to methodological limitations in detecting and quantifying these smaller particles, which are often more difficult to capture or analyze accurately. Nevertheless, smaller MPs are more mobile and can be more readily inhaled, posing potential health risks if not effectively filtered or removed from indoor environments. This size distribution suggests that indoor MPs are generally larger, likely reflecting the types of activities, materials, and sources contributing to indoor contamination, such as dust, textiles, and plastic-based products. The relative stability in the proportions of specific size fractions, particularly the 100–250 μm, 250–500 μm, and 500–1000 μm ranges, may indicate the presence of persistent sources or limited degradation of these particles in indoor environments. Although these larger MPs are less susceptible to rapid degradation, they can remain suspended in air or accumulate on surfaces, thereby contributing to the long-term buildup of microplastic pollution indoors.

The morphological analysis of indoor airborne microplastics revealed a clear dominance of fibrous particles, which accounted for an average of 66 % of all identified microplastics, while fragments constituted approximately 34 %. The proportions of fibers and fragments fluctuated over time. For instance, during December 11–25, 2023, fragments represented 23 %, whereas fibers comprised 77 %. These proportions varied across sampling periods, indicating temporal changes in MP types. For example, during February 12–19, 2024, the fragment percentage increased to 42 %, while the fiber percentage decreased to 58 %.

3.1.2.2. Outdoor. The size distribution of MPs in the indoor environment also exhibited temporal variability across the analyzed periods (Fig. 5). For the smallest size category (<50 μm), the proportion of MPs remained consistently low, below 2 % on average, with the highest recorded value of 3 % observed on January 1, 2024. In contrast, MPs within the 50–100 μm range showed greater

fluctuation but generally accounted for more than 30 %, reaching a peak of 54 % during February 12–19, 2024. The most dominant size class throughout the study was the 100–250 μm range, which consistently accounted for more than 40 % of the detected MPs and peaked at 54 % during March 18–25, 2024. Overall, these findings suggest that medium-sized particles are prevalent in outdoor environments and may originate from sources such as vehicle emissions, industrial activities, or the atmospheric transport of larger particles from distant regions. Particles within the 250–500 μm range in the outdoor environment represent a moderate fraction of the total MPs, consistently accounting for approximately 10–30 % of the overall particle count across the different sampling periods. While this size class exhibited relatively stable proportions, some fluctuations were noted. Notable peaks occurred on January 9, 2024, and during March 18–25, 2024, with both periods recording a maximum contribution of 30 %. These MPs are typically composed of particles large enough to be detected, yet small enough to be transported over long distances by wind or water currents. They likely originate from multiple sources, including the fragmentation of larger plastic debris, such as plastic packaging, plastic containers, and larger plastic products, as well as from industrial processes that produce plastic products in this size range. MPs in the 500–1000 μm size range showed relatively low percentages, with the highest observed value being 5 % during March 18–25, 2024. Similarly, MPs larger than 1000 μm consistently represented a very small fraction of the total, although occasional fluctuations occurred. For instance, during the same March 18–25 period, particles > 1000 μm accounted for 8 % of total MPs, the highest for this category. These larger particles are less likely to remain airborne due to their greater mass and are typically associated with local sources such as fragmented plastic waste. Nonetheless, these particles may become temporarily suspended under certain meteorological conditions, such as strong winds, or may be resuspended by mechanical disturbances. According to Hale et al. (2020), such variability in the occurrence of large airborne MPs may reflect episodic events or processes, including increased fragmentation of macroplastics, variations in source inputs, or environmental factors such as wind speed, direction, and surface roughness.

The shape distribution of MPs showed a clear dominance of fragments over fibers throughout most of the sampling periods. Fragments consistently constituted the majority of detected MPs, with the highest proportion recorded during March 18–25, 2024, when they represented 94 % of the total particles. In contrast, fibers represented a smaller but persistent fraction of the total MPs count. The highest percentage of fibers was observed during the period of February 1–6, 2024, reaching their highest proportion of 25 % during February 1–6, 2024.

Across all size categories, black MPs demonstrated a consistent presence; however, their relative proportion generally decreased with decreasing particle size, except in the smallest size class (<50 μm), where their presence remained notable. A strong correlation ($r = 0.7$) was observed between black MPs and the 100–250 μm size range, suggesting that black particles are more commonly associated with these larger size ranges. Brown MPs also exhibited a significant correlation across all size categories, indicating a widespread distribution pattern independent of particle size. These consistent associations may reflect the broad range of sources contributing to black and brown MPs, as well as their material properties that influence fragmentation behavior and atmospheric transport.

White MPs showed a notable correlation within the 50–100 μm size category, potentially reflecting distinct pollution pathways such as the fragmentation of consumer products, packaging materials, or lightweight synthetic polymers. In contrast, brown MPs exhibited a stronger correlation with the 250–500 μm range, which may indicate origins from agricultural materials, dyed textiles, or organic contamination associated with soil or plant debris. The occurrence of blue, green, and red MPs was relatively limited across all size categories, suggesting that these colors are either less prevalent in the studied environment or are indicative of specific, less

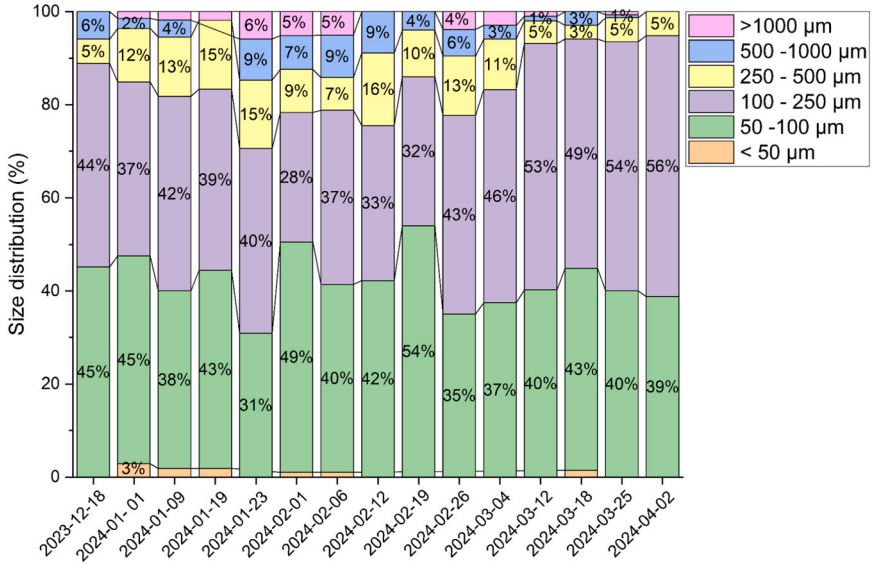

Fig. 5. Size distribution of microplastics collected in outdoor air. The data are categorized into five size bins: < 50 μm, 50–100 μm, 100–250 μm, 250–500 μm, and 500–1000 μm. The y-axis represents the percentage of total MPs falling within each size category.

dominant sources. Their sporadic presence may be linked to isolated activities or materials (e.g., colored clothing fibers, decorative plastics) rather than continuous or widespread emission sources.

3.1.3. Chemical composition

The chemical characterization of MPs revealed a heterogeneous mixture of polymer types indoor, reflecting diverse material sources and usage patterns within enclosed spaces. Among the identified polymers, PES was consistently dominant indoors, comprising 33.0 % of all analyzed particles. (Fig. 6). Acrylates followed closely at 31.1 %, together accounting for 64.1 % of indoor MPs. These polymers are commonly associated with synthetic textiles, furniture coatings, and household products, suggesting that indoor sources are largely driven by human activities, including fabric abrasion, material degradation, and the use of treated surfaces primary drive indoor sources. PE, although dominant outdoors, accounted for only 16,0 % indoors. The presence of nitrile rubber (6,7 %) further supports the influence of indoor-specific sources such as flooring materials, gloves, or sealants. The presence of PP (3.8 %), PS (4.7 %), and smaller amounts of polyisoprene (2.8 %) and PVC (1.9 %) further supports a range of indoor-specific sources including flooring materials, packaging, sealants, and textiles.

In contrast to indoor air, the outdoor environment was characterized by a strong dominance of PE, comprising ~48.6 % of the total detected MPs. This prevalence is likely attributable to the widespread environmental degradation of plastic packaging, bags, and other polyethylene-based debris. Other notable polymers identified in the outdoor air included polyester (PES, 11.9 %), acrylates (10.8 %), and nitrile rubber (10.4 %), suggesting additional contributions from airborne textile fibers, weathered paints or coatings, and traffic-related sources. Furthermore, polymers such as PP (7.7 %), PS (7.5 %), PA (1.4 %) and PVC (1.0 %) were observed in higher relative proportions in outdoor samples compared to indoor environment. These differences may reflect the impact of environmental weathering, atmospheric transport, and exposure conditions on polymer fragmentation and persistence. Of polymers

The presence of shared polymers, such as PE and PES in both environments suggests strong cross-contamination or shared emission sources, due to air exchange and the fragmentation potential of these polymers.

3.1.4. Microplastic source attribution

A comparison of airborne MP sources in indoor and outdoor environments reveals distinct profiles (Fig. 7). In the indoor

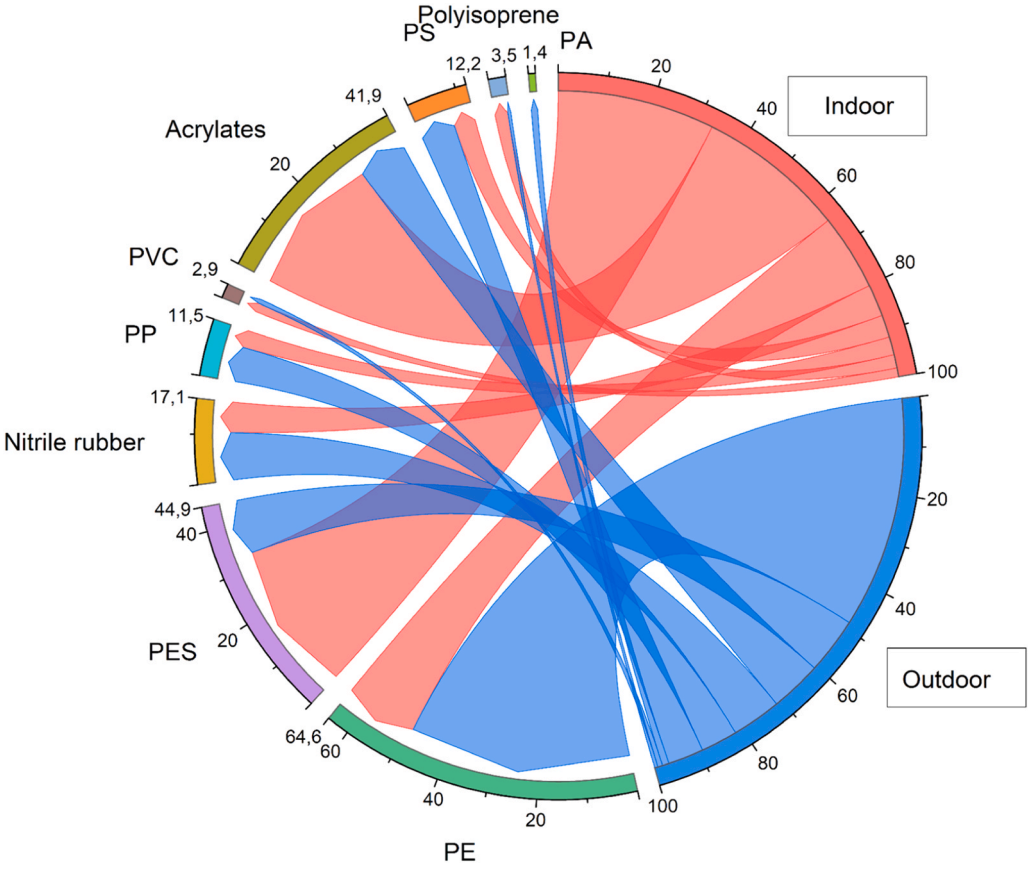

Fig. 6. Chemical composition of MPs indoors and outdoors. Chord diagram showing how indoor (red) and outdoor (blue) environments contribute to the observed polymer types; ribbon width is proportional to contribution. Minor cross-links indicate polymers present in both environments but with different magnitudes. Numbers on arcs denote shares (%).

environment, the largest share of MPs was attributed to textile-related sources, accounting for 31 % of the total. This predominance is consistent with the known shedding of synthetic fibers from clothing, upholstery, curtains, and carpets (Dris et al., 2017). Our indoor–outdoor contrast (fibers dominant indoors; PE/PP and fragments prevalent outdoors) aligns with classroom deposition studies in universities, which also report fiber dominance (average sizes ~120–2222 μm) and polymers linked to textiles/fixtures (e.g., PA6/PA12, PP) (Bhat, 2024b), The confined nature of indoor spaces facilitates the accumulation and suspension of textile fibers in the air. Packaging materials contributed 30.6 %, likely originating from the handling and degradation of plastic containers, bags, and wrappers frequently used and stored indoors. Notably, this category exhibited the greatest variability among all sources (range = 14.2 %), with peak contributions aligning temporally with elevated fragment abundance and higher proportions of PP and PE. This suggests that packaging-derived MPs are episodically released, likely influenced by daily activities such as handling or unpacking plastic materials. MPs derived from flooring materials represented 17.3 %, suggesting a significant contribution from abrasion of plastic-based floor coverings, composite panels, and sealants. Higher values in samples were enriched with PVC, rubber-based polymers, and larger particle size classes (>500 μm). This reflects potential inputs from surface abrasion of vinyl flooring, rubber mats, or foot traffic-induced resuspension of settled debris. While the average contribution was the lowest among all sources, the observed range (13.9 %–21.4 %) suggests that flooring may act as an episodic reservoir for MP release. Notably, outdoor-derived particles constituted 21.1 %, indicating the infiltration of microplastics from the external environment through ventilation systems, open windows, or via occupants.

The outdoor microplastic source attribution analysis revealed a markedly different source profile compared to indoor environments (Fig. 7). The outdoor MP profile was dominated by packaging-related sources, which comprised 46.3 % (from 40.4 % to 66.0 %) of the total, primarily driven by high levels of PE and PP fragments (Dris et al., 2016b). This reflects the widespread environmental dispersion of fragmented plastic debris such as bags, films, and containers subjected to weathering, UV degradation, and mechanical breakdown. MPs of outdoor origin, including those from road dust, tire wear, and soil-bound fragments, represented 28.1 % (from 21.4 % to 30.9 %), emphasizing the influence of urban infrastructure and vehicular activity. This category was strongly associated with black coloration, large fragments, and rubber-based polymers such as polyisoprene and synthetic rubbers. Flooring-related MPs, potentially arising from wear of outdoor surfaces or construction materials, accounted for 16 % (from 9.5 % to 20.0 %). Although indoor floors are unlikely to be a direct source of outdoor particles, urban analogs such as painted façades, outdoor linings, or degraded construction materials may contribute similar particles. Textile-derived MPs accounted for only 9.6 % (ranging from 3.1 % to 11.6 %) of the total, which is substantially lower than the indoor levels, supporting the hypothesis that textile fiber emissions are predominantly localized within enclosed environments. These values are consistent with expectations that synthetic textile fibers, while abundant indoors, are far less prevalent or persistent in the more turbulent and diluted outdoor air environment. The Linear discriminant analysis (LDA) model achieved a perfect classification accuracy of 100 % using cross-validation, successfully separating indoor and outdoor MPs profiles based solely on their estimated source contributions (Textiles, packaging, flooring, outdoors) (Fig. 8).

The LD1 axis clearly discriminates between the two environments. Indoor samples are characterized by higher textile-related input, while outdoor samples are dominated by packaging and environmental sources. This result confirms that source composition alone is sufficient to accurately distinguish environmental origin, validating the attribution model and its interpretive power.

Sensitivity tests indicate our indoor vs. outdoor apportionment results remain unchanged under ±20 % perturbations. Three complementary approaches were applied including one-at-a-time perturbations (±20 %) of individual weighting rows showed only modest shifts (<5–6 % on average) in source contributions. Leave-one-feature-out tests (removing morphology, size, or color) slightly altered the relative importance of packaging, but textiles consistently remained the dominant indoor source. Dirichlet Monte Carlo resampling (2000 simulations) generated 95 % confidence intervals and probabilities of source dominance. Indoors, Textile source were dominant in > 85 % of runs, while outdoors, Packaging and Outdoor categories alternated as top contributors. The sensitivity tests demonstrated that the apportionment results are robust to reasonable variations in the weighting scheme, supporting the validity of the observed trends.

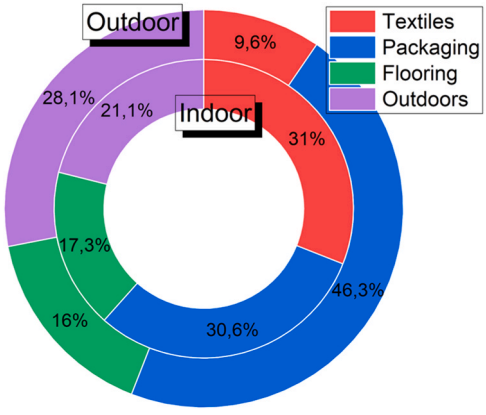

Fig. 7. Microplastic Source Attribution Map.

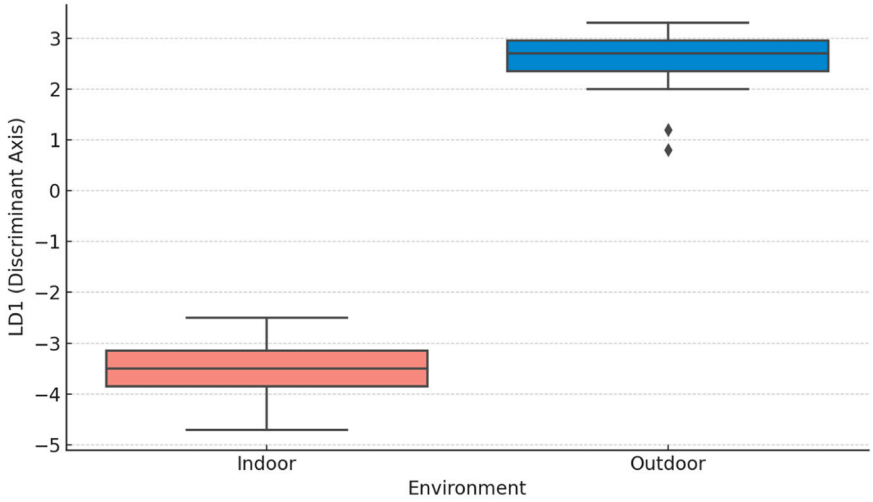

Fig. 8. Linear discriminant analysis.

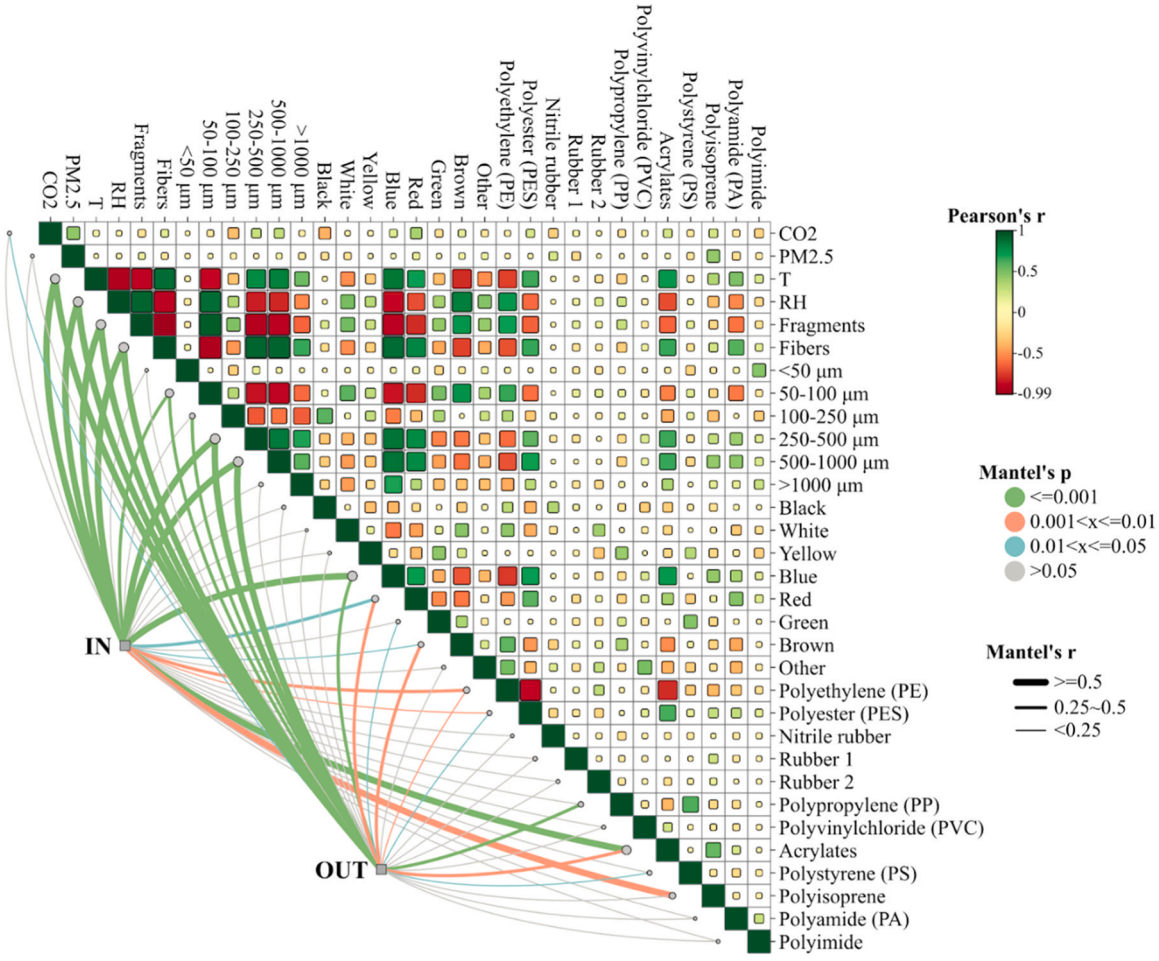

Fig. 9. Mantel test heatmap network analysis of the relationship between indoor and outdoor MP concentrations, their physicochemical characteristics, and environmental parameters.

3.2. Indoor - Outdoor relationship analysis

3.2.1. Mantel test

To evaluate the degree of similarity between indoor and outdoor MPs pollution profiles, a Mantel test was conducted comparing particle characteristics and environmental parameters. The results, visualized in a chord-like network diagram (Fig. 9), revealed statistically significant correlations between indoor and outdoor MP profiles.

The Mantel correlation coefficients demonstrated that many MPs variables, particularly polymer types and particle size fractions, exhibited moderate to strong similarity ($r \geq 0.5$) between indoor and outdoor environments. A high number of green-colored connections ($p \leq 0.001$) indicates robust statistical significance, suggesting that outdoor microplastic pollution is a major contributor to indoor MP presence. This supports the hypothesis of air exchange-driven transfer, particularly in investigated urban settings with high particulate loads and insufficient filtration. Notably, MP types such as fibers and fragments, as well as several size fractions (250–500 μm, 500–1000 μm, and >1000 μm), showed strong correlations (Mantel's $r \geq 0.5$), suggesting that outdoor air serves as a key source of indoor MPs. The results are consistent with other studies that have shown the presence of fibers and fragments in indoor environments, where synthetic fibers are easily torn and separated from indoor sources like clothing, carpets, and curtains (Nematollahi et al., 2022). High correlation coefficients were observed for polymers such as PP, PE, and PS, which are commonly found in urban air due to widespread use in textiles and packaging. These results indicate that both ambient infiltration and internal re-emission as key pathways for the presence of indoor MP. Specific particle types and polymers were significantly associated with environmental variables. Pearson correlation analysis showed no significant correlation between $PM_{2.5}$ and Meanwhile, a weak correlation was observed between CO_2 levels and outdoor MP concentrations ($r = 0.16$, $p < 0.05$), which we interpret cautiously as not evidencing a causal link. CO_2 and $PM_{2.5}$ concentrations were positively correlated with MP abundance, particularly for black and white MPs and polymers such as PP, PES, and PS, suggesting links to anthropogenic activity and traffic non-combustion-related emissions. The significant correlation between indoor MPs and acrylates highlights synthetic fibers as a key source of indoor microplastic pollution. In colder countries, where thicker, layered clothing is often worn to stay warm, the increased use of synthetic fabrics likely contributes to higher levels of microplastic shedding indoors. Relative humidity was moderately correlated with smaller MPs and fibers, possibly due to enhanced deposition and reduced resuspension under humid conditions. The findings emphasize the need for integrated air quality and microplastic mitigation strategies, particularly in public buildings where vulnerable populations (e.g., children) are present.

While both environments show morphological and polymer-based differentiation, indoor samples exhibit more variation in fiber-rich materials and mid-sized colored particles, reflecting textile wear and indoor activity. Conversely, outdoor samples are more strongly influenced by fragmented packaging and tire-derived particles, with fiber contributions appearing sporadically and at lower levels. This comparison underscores the distinct source regimes operating indoors and outdoors: indoors dominated by continuous textile shedding with episodic synthetic material inputs, and outdoors shaped by urban environmental fragmentation, resuspension, and outdoor air transport processes. PCA thus serves as a powerful tool to distinguish these overlapping but environmentally specific microplastic signatures.

3.2.2. Rubber sources analysis

Fourier-transform infrared spectroscopy was employed to investigate the chemical composition of three rubber samples, revealing distinct spectral features that enable tentative source identification. The spectral features suggest that each rubber type may originate from different product categories, reflecting differences in polymer composition and the use of additives. Rubber 1 exhibited a strong absorption band at 1740 cm^{-1} , attributed to C═O stretching vibrations of ester or carboxylic acid groups, along with a broad absorption region between 1470 and 1300 cm^{-1} , indicative of C–H bending and C–O stretching modes. The presence of pronounced polar functional groups indicates that the materials contain plasticizers or ester-modified polymers. This profile is consistent with synthetic rubbers used in consumer products where flexibility and water resistance are important. In addition to waterproof footwear such as rubber or PVC boots, potential sources may include synthetic leather goods, rubberized floor coverings, or automotive interior components (e.g., door seals or dashboard coatings). Rubber 2 displayed absorption bands at 1550, 1470, 1390, and 1250 cm^{-1} , accompanied by weaker peaks at 1750 and 1650 cm^{-1} . These features indicate a vulcanized rubber formulation with aromatic and weakly polar functionalities, suggesting the presence of additives or co-monomers such as nitrile, acrylonitrile, or aromatic ring structures. Such compositions are typical of technical rubbers used in both industrial and consumer applications. Potential sources therefore include the soles of work or hiking boots, industrial gloves, rubber gaskets, hoses, or belts, as well as internal tire components such as sidewalls or inner liners, where more chemically resistant rubber compounds are used. Rubber 3, in contrast, showed peaks at 1550, 1470, and 1370 cm^{-1} , without any significant carbonyl absorptions in the 1700–1750 cm^{-1} region. The absence of polar groups, combined with vibrations consistent with aromatic C═C and aliphatic C–H modes, indicates a predominantly hydrocarbon-based material. This is characteristic of non-polar rubbers such as styrene-butadiene rubber (SBR), butadiene rubber (BR), or natural rubber (NR), which are extensively used in applications requiring mechanical durability and wear resistance. The most probable source of Rubber 3 is vehicle tire tread, although similar formulations may also be found in industrial conveyor belts, rubber bands, sports shoe outsoles, or anti-vibration components. Indoors in most samples nitrile butadiene rubber (a synthetic copolymer widely used for its oil and chemical resistance) was found. It may originate primarily from disposable gloves used by cleaning or food service staff, as well as from rubber soles of staff and student footwear. Additional sources include seals and gaskets in HVAC systems or maintenance equipment. Over time, mechanical wear and surface abrasion can lead to the release of NBR particles, contributing to indoor particulate matter of synthetic origin.

3.2.3. Inhalation hazard-weighted abundance risk

Analysis of the IHWAI revealed clear and quantifiable differences in MPs hazard potential between indoor and outdoor environments. Indoor samples consistently exhibited higher IHWAI values, with a pronounced peak observed during the sampling period of February 26 – March 4, 2024, when the index reached 284.68. This high IHWAI score was driven by a fibrous particle proportion of 59.86 %, alongside significant shares of PES (32.59 %), rubber (5.73 %), and polyamide (3.70 %), all polymers associated with elevated toxicological profiles and respiratory persistence. The episode likely reflects an acute indoor pollution event, potentially linked to the shedding of textiles or the resuspension of degraded synthetic materials. In contrast, outdoor samples displayed markedly lower and more stable IHWAI profiles, with values ranging from 229.41 to 246.83, and normalized scores between 0.10 and 0.20, compared to indoor peaks normalized to 1.00. Outdoor samples were overwhelmingly dominated by fragments (typically >85 %) and low-risk polymers such as PE and PP - reaching as high as 95.45 % PE (January 1–9, 2024) and 100 % PE (March 18–25, 2024). The low fiber content, often below 10 %, substantially reduced their shape-weighted risk contributions, even when the total microplastic deposition exceeded 6000 MP/m^2/day, as observed on March 4–12, 2024. The maximum IRI observed across all samples was 383.81, recorded in the outdoor air on February 6–12, 2024. This unusually high outdoor value was driven by a combination of elevated fiber content (25.25 %) and substantial contributions from high-hazard polymers such as PES (33.33 %), PVC (11.11 %), PS (11.11 %), and PA (11.11 %). This indicates a rare outdoor pollution event involving multiple high-risk microplastic types, however, this difference should not be interpreted as a quantitative health risk as does not incorporate inhaled dose, size-dependent deposition, or dose–response.

4. Conclusions

This study provides a comprehensive assessment of airborne microplastics (MPs) in a school environment through an integrated framework combining quantitative measurements, multi-attribute source apportionment, and inhalation hazard-weighted abundance evaluation. The semi-quantitative source apportionment model identified four main indoor MP contributors - textiles (31.0 %), packaging (30.6 %), flooring (17.3 %), and outdoor infiltration (21.1 %). Textile fibers were consistently dominant indoors, highlighting continuous shedding from synthetic clothing and soft furnishings. Packaging-related MPs occurred episodically, linked to occupant activity and material handling, while flooring-derived particles, particularly from PVC and rubber composites-originated both through abrasion and resuspension. In contrast, outdoor MP profiles were dominated by packaging-related sources (46.3 %) and transport-derived particles (28.1 %), particularly polyethylene and rubber fragments associated with urban pollution, tire wear, and degraded plastic litter. Textile-derived MPs were comparatively scarce outdoors, underscoring their limited persistence in turbulent and ventilated environments.

Color distribution revealed a dominance of black MPs both indoors (53 %) and outdoors (>50 %), associated with tire wear and dark-colored textiles. Blue MPs were the second most abundant indoors (26 %), while white MPs were more prevalent outdoors (~10 %), reflecting contributions from packaging and consumer plastic debris. Less frequent colors (yellow, brown, red, and green) occurred sporadically, indicating episodic or source-specific emissions.

Size and morphology analysis showed that medium-sized particles (100–250 μm) predominated in both environments, contributing over 30–40 % of total MPs. Indoors, larger fractions (250–1000 μm) were consistently present, indicating continuous inputs from textile abrasion, flooring materials, and dust resuspension. Smaller MPs (<50 μm) comprised less than 2 %, likely due to detection limits and filtration efficiency. Fibers dominated indoors (~66 %), while fragments prevailed outdoors (>90 %), reflecting differences in source types and atmospheric dynamics.

Chemical composition revealed distinct environmental signatures, with indoor air dominated by PES (33.0 %) and ACR (31.1 %), while outdoor samples were enriched in PE (48.6 %) and PP (7.7 %). Mantel test results ($r \geq 0.5$, $p \leq 0.001$) confirmed statistically significant correlations between indoor and outdoor MP profiles, especially for common polymers (PE, PP, PS) and coarser size fractions (250–500 μm, 500–1000 μm, >1000 μm), emphasizing strong indoor–outdoor exchange.

The inhalation hazard-weighted abundance index IHWAI, a unitless, comparative metric developed in this study by combining REACH/CLP-based polymer-weightings with MPs morphology, identified elevated index values in samples enriched in PVC, rubber-based polymers, and fibrous MPs. Indoor air was found to carry a more diverse and comparatively higher-weighted profile, reflecting the prevalence of fibrous particles and polymers used in flooring and treated textiles. Although unitless and non-dose-specific, the IHWAI framework offers a practical tool to rank samples by hazard-weighted composition using REACH/CLP-based polymer weighting and morphology. These findings suggest that indoor environments may pose a disproportionately higher inhalation hazard due to the dominance of fibrous and high-weighted polymer particles.

Mitigation should target both outdoor and indoor sources. Outdoors, actions should focus on reducing MPs emissions from tire wear and litter through improved street cleaning, dust management, and the adoption of low-wear materials. Indoors, mitigation requires replacing high-shedding synthetic materials with low-emission or natural alternatives and enhancing ventilation and filtration systems. Standardized, size-resolved methods and multi-city datasets are essential to establish evidence-based benchmarks and guide policy development toward healthier school environments.

CRediT authorship contribution statement

Ieva Uogintė: Writing – review & editing, Visualization, Methodology, Formal analysis, Data curation. **Lina Davulienė:** Validation, Methodology, Investigation. **Sergej Šemčuk:** Investigation, Formal analysis. **Mehri Davtalab:** Writing – review & editing, Visualization, Software. **Steigvilė Byčenkienė:** Writing – original draft, Supervision, Project administration, Funding acquisition,

Data curation, Conceptualization. **Mario Lovrić:** Writing – review & editing, Visualization. **Vadimas Dudoitis:** Validation, Methodology. **Simonas Kecorius:** Writing – review & editing, Methodology.

Declaration of Competing Interest

The authors declare that they have no known competing financial interests or personal relationships that could have appeared to influence the work reported in this paper.

Acknowledgment

This project (EDIAQI) has received funding from the European Union's Horizon Europe research and innovation programme under grant agreement No. 101057497.

Data availability

Data will be made available on request.

References

"EDIAQI Project - Evidence driven indoor air quality improvement." Accessed: Jul. 09, 2025. [Online]. Available: https://ediaqi.eu/.
Abbasi, S., Turner, A., Sharifi, R., Nematollahi, Mohammad J., Keshavarzifard, M., Moghtaderi, T., 2022. Microplastics in the school classrooms of Shiraz, Iran (Jan). Build. Environ. 207, 108562. https://doi.org/10.1016/j.buildenv.2021.108562.
Al-Hussayni, R.S., Al-Ahmady, K.K., Mhemid, R.K.S., 2023. Assessment of indoor microplastic particles pollution in selected sites of Mosul city (Sep). J. Ecol. Eng. 24 (9), 322–332. https://doi.org/10.12911/22998993/168461.
Allen, S., et al., 2019a. Atmospheric transport and deposition of microplastics in a remote mountain catchment. vol. 12, no. 5, pp. 339–344, Apr Nat. Geosci. 12 (5). https://doi.org/10.1038/s41561-019-0335-5.
Allen, S., et al., 2019b. Atmospheric transport and deposition of microplastics in a remote mountain catchment. vol. 12, no. 5, pp. 339–344, Apr Nat. Geosci. 12 (5). https://doi.org/10.1038/s41561-019-0335-5.
Arvaniti, O.S., et al., 2022. Effectiveness of tertiary treatment processes in removing different classes of emerging contaminants from domestic wastewater (Nov). Front. Environ. Sci. Eng. 16 (11), 148. https://doi.org/10.1007/s11783-022-1583-y.
Bhat, M.A., 2024b. Microplastics in indoor deposition samples in university classrooms (Mar). Discov. Environ. 2 (1), 23. https://doi.org/10.1007/s44274-024-00054-0.
Bhat, M.A., 2024a. Indoor microplastics and microfibers. Microfibre Pollution from Textiles. CRC Press, Boca Raton, pp. 285–307. https://doi.org/10.1201/9781003331995-16.
Bhat, M.A., 2024a. Airborne microplastic contamination across diverse university indoor environments: A comprehensive ambient analysis (Sep). Air Qual. Atmos. Health 17 (9), 1851–1866. https://doi.org/10.1007/s11869-024-01548-9.
Chakraborty, S., Banerjee, M., Jayaraman, G., Rajeswari V, D., 2024. Evaluation of the health impacts and deregulation of signaling pathways in humans induced by microplastics (Dec). Chemosphere 369, 143881. https://doi.org/10.1016/J.CHEMOSPHERE.2024.143881.
Chen, G., Feng, Q., Wang, J., 2020. Mini-review of microplastics in the atmosphere and their risks to humans (Feb). Sci. Total Environ. 703, 135504. https://doi.org/10.1016/J.SCITOTENV.2019.135504.
Chenappan, N.K., et al., 2024. Quantification and characterization of airborne microplastics in the coastal area of Terengganu, Malaysia (Mar). Environ. Monit. Assess. 196 (3), 1–15. https://doi.org/10.1007/S10661-024-12381-Z/METRICS.
Cui, Y., et al., 2025. Mitigating microplastic-induced organ Damage: Mechanistic insights from the microplastic-macrophage axes (Jul). Redox Biol. 84, 103688. https://doi.org/10.1016/J.REDOX.2025.103688.
Dewika, M., et al., 2025. Assessing the concentration, distribution and characteristics of suspended microplastics in the Malaysian indoor environment (Jan). Sci. Total Environ. 959, 178049. https://doi.org/10.1016/j.scitotenv.2024.178049.
Dris, R., et al., 2017. A first overview of textile fibers, including microplastics, in indoor and outdoor environments (Feb). Environ. Pollut. 221, 453–458. https://doi.org/10.1016/j.envpol.2016.12.013.
Dris, R., Gasperi, J., Saad, M., Mirande, C., Tassin, B., 2016b. Synthetic fibers in atmospheric fallout: a source of microplastics in the environment? (Mar). Mar. Pollut. Bull. 104 (1–2), 290–293. https://doi.org/10.1016/j.marpolbul.2016.01.006.
Dris, R., Gasperi, J., Saad, M., Mirande, C., Tassin, B., 2016a. Synthetic fibers in atmospheric fallout: a source of microplastics in the environment? (Mar). Mar. Pollut. Bull. 104 (1–2), 290–293. https://doi.org/10.1016/J.MARPOLBUL.2016.01.006.
Education at a Glance 2023 Sources, methodologies and technical notes," Education at a Glance 2023 Sources, Methodologies and Technical Notes, Sep. 2023, doi: 10.1787/D7F76ADC-EN.
Ferraz, G.M., dos, A., de Moraes, S., dos Santos, G.B., de Miranda, I.T., Zucolotto, V., Urban, R.C., 2024. Atmospheric microplastics deposition assessment in a countryside municipality in Southeastern Brazil: a case study at a state elementary school (Dec). Chemosphere 369, 143886. https://doi.org/10.1016/j.chemosphere.2024.143886.
Hale, R.C., Seeley, M.E., La Guardia, M.J., Mai, L., Zeng, E.Y., 2020. A global perspective on microplastics. p. e2018JC014719, Jan J. Geophys Res Oceans 125 (1). https://doi.org/10.1029/2018JC014719.
Huang, Y., et al., 2021. Atmospheric transport and deposition of microplastics in a subtropical urban environment (Aug). J. Hazard Mater. 416, 126168. https://doi.org/10.1016/J.JHAZMAT.2021.126168.
Jenner, L.C., Rotchell, J.M., Bennett, R.T., Cowen, M., Tentzeris, V., Sadofsky, L.R., 2022. Detection of microplastics in human lung tissue using μFTIR spectroscopy (Jul). Sci. Total Environ. 831, 154907. https://doi.org/10.1016/j.scitotenv.2022.154907.
K C, P.B., et al., 2023. Polytetrafluorethylene microplastic particles mediated oxidative stress, inflammation, and intracellular signaling pathway alteration in human derived cell lines (Nov). Sci. Total Environ. 897, 165295. https://doi.org/10.1016/J.SCITOTENV.2023.165295.
Kek, H.Y., et al., 2024. Critical review on airborne microplastics: an indoor air contaminant of emerging concern (Mar). Environ. Res. 245, 118055. https://doi.org/10.1016/j.envres.2023.118055.
Knobloch, E., Ruffell, H., Aves, A., Pantos, O., Gaw, S., Revell, L.E., 2021. Comparison of deposition sampling methods to collect airborne microplastics in Christchurch, New Zealand (Apr). Water Air Soil Pollut. 232 (4), 1–10. https://doi.org/10.1007/S11270-021-05080-9/METRICS.
Kumar, R., et al., 2025. Nanotoxicity unveiled: evaluating exposure risks and assessing the impact of nanoparticles on human health (Sep). J. Trace Elem. Miner. 13, 100252. https://doi.org/10.1016/J.JTEMIN.2025.100252.
Liu, K., Wang, X., Fang, T., Xu, P., Zhu, L., Li, D., 2019b. Source and potential risk assessment of suspended atmospheric microplastics in Shanghai (Jul). Sci. Total Environ. 675, 462–471. https://doi.org/10.1016/J.SCITOTENV.2019.04.110.

Liu, K., Wang, X., Fang, T., Xu, P., Zhu, L., Li, D., 2019a. Source and potential risk assessment of suspended atmospheric microplastics in Shanghai (Jul). Sci. Total Environ. 675, 462–471. https://doi.org/10.1016/J.SCITOTENV.2019.04.110.
Liu, J., Zheng, L., 2025. Microplastic migration and transformation pathways and exposure health risks (Mar). Environ. Pollut. 368, 125700. https://doi.org/10.1016/j.envpol.2025.125700.
Luo, Q., et al., 2025. Microplastics as an emerging threat to human health: an overview of potential health impacts (Jul). J. Environ. Manag. 387, 125915. https://doi.org/10.1016/J.JENVMAN.2025.125915.
Marfella, R., et al., 2024. Microplastics and nanoplastics in atheromas and cardiovascular events (Mar). N. Engl. J. Med. 390 (10), 900–910. https://doi.org/10.1056/NEJMoa2309822.
Materić, D., et al., 2020. Micro-and nanoplastics in alpine snow: a new method for chemical identification and (semi)quantification in the nanogram range (Feb). Environ. Sci. Technol. 54 (4), 2353–2359. https://doi.org/10.1021/ACS.EST.9B07540/SUPPL_FILE/ES9B07540_SI_005.ZIP.
Maurizi, L., Simon-Sánchez, L., Vianello, A., Nielsen, A.H., Vollertsen, J., 2024. Every breath you take: high concentration of breathable microplastics in indoor environments (Aug). Chemosphere 361, 142553. https://doi.org/10.1016/j.chemosphere.2024.142553.
McCormack, M., et al., 2018. School environment, indoor air quality, student performance and health. vol. 2018, no. 1, Sep ISEE Conf. Abstr.. https://doi.org/10.1289/isesisee.2018.S03.01.15.
Morioka, T., Tanaka, S., Kohama-Inoue, A., Watanabe, A., 2024. The quantification of the airborne plastic particles of 0.43–11 μm: procedure development and application to atmospheric environment (Mar). Chemosphere 351, 141131. https://doi.org/10.1016/J.CHEMOSPHERE.2024.141131.
Nandi, S., Kumar, R.N., Dhandapani, A., Iqbal, J., 2024. Characterization of microplastics in outdoor and indoor air in Ranchi, Jharkhand, India: first insights from the region (Apr). Environ. Pollut. 346, 123543. https://doi.org/10.1016/J.ENVPOL.2024.123543.
Nematollahi, M.J., et al., 2022. Microplastic occurrence in settled indoor dust in schools (Feb). Sci. Total Environ. 807, 150984. https://doi.org/10.1016/J.SCITOTENV.2021.150984.
Nihart, A.J., et al., 2025. Bioaccumulation of microplastics in decedent human brains (Apr). Nat. Med. 31 (4), 1114–1119. https://doi.org/10.1038/s41591-024-03453-1.
Niu, S., et al., 2024. Quantifying the chemical composition and real-time mass loading of nanoplastic particles in the atmosphere using aerosol mass spectrometry (Feb). Environ. Sci. Technol. 58 (7), 3363–3374. https://doi.org/10.1021/ACS.EST.3C10286/ASSET/IMAGES/LARGE/ES3C10286_0005.JPEG.
O'Leary, K., 2024. Health impacts of microplastic exposure. vol. 30, no. 12, pp. 3392–3392, Dec Nat. Med. 30 (12). https://doi.org/10.1038/s41591-024-03388-7.
Pathak, D., 2025. Enemies of the hormones: microplastics and endocrine disruptors impacting public health (Jan). Health Clim. Chang. Unravel. Connect. 119–150. https://doi.org/10.1016/B978-0-443-29240-8.00014-6.
Pomata, D., et al., 2024. Plastic breath: Quantification of microplastics and polymer additives in airborne particles (Jul). Sci. Total Environ. 932, 173031. https://doi.org/10.1016/j.scitotenv.2024.173031.
Sharma, N., et al., 2024. Microplastic residues in clinical samples: a retrospection on sources, entry routes, detection methods and human toxicity. Trends Anal. Chem. 173, 117618. https://doi.org/10.1016/j.trac.2024.117618.
Szewc, K., Graca, B., Dołęga, A., 2021. Atmospheric deposition of microplastics in the coastal zone: characteristics and relationship with meteorological factors (Mar). Sci. Total Environ. 761, 143272. https://doi.org/10.1016/J.SCITOTENV.2020.143272.
U.S. EPA. Ambient Monitoring Guidelines for Prevention of Significant Deterioration (PSD), EPA-450/4-87-007. Office of Air Quality Planning and Standards, Research Triangle Park, NC.
Vianello, A., Jensen, R.L., Liu, L., Vollertsen, J., 2019b. Simulating human exposure to indoor airborne microplastics using a breathing thermal manikin (Jun). Sci. Rep. 9 (1), 8670. https://doi.org/10.1038/s41598-019-45054-w.
Vianello, A., Jensen, R.L., Liu, L., Vollertsen, J., 2019a. Simulating human exposure to indoor airborne microplastics using a breathing thermal manikin. vol. 9, no. 1, pp. 1–11, Jun Sci. Rep. 9 (1). https://doi.org/10.1038/s41598-019-45054-w.
Wang, M., Wu, Y., Li, G., Xiong, Y., Zhang, Y., Zhang, M., 2024. The hidden threat: unraveling the impact of microplastics on reproductive health (Jul). Sci. Total Environ. 935, 173177. https://doi.org/10.1016/J.SCITOTENV.2024.173177.
Wright, S.L., Kelly, F.J., 2017. Plastic and human health: a micro issue? (Jun). Environ. Sci. Technol. 51 (12), 6634–6647. https://doi.org/10.1021/ACS.EST.7B00423/SUPPL_FILE/ES7B00423_SI_001.PDF.
Wright, S.L., Ulke, J., Font, A., Chan, K.L.A., Kelly, F.J., 2020. Atmospheric microplastic deposition in an urban environment and an evaluation of transport (Mar). Environ. Int. 136, 105411. https://doi.org/10.1016/J.ENVINT.2019.105411.
Yukioka, S., et al., 2020. Occurrence and characteristics of microplastics in surface road dust in Kusatsu (Japan), Da Nang (Vietnam), and Kathmandu (Nepal) (Jan). Environ. Pollut. 256, 113447. https://doi.org/10.1016/J.ENVPOL.2019.113447.
Zarus, G.M., Muianga, C., Hunter, C.M., Pappas, R.S., 2021. A review of data for quantifying human exposures to micro and nanoplastics and potential health risks (Feb). Sci. Total Environ. 756, 144010. https://doi.org/10.1016/j.scitotenv.2020.144010.
Zhai, X., Zheng, H., Xu, Y., Zhao, R., Wang, W., Guo, H., 2023. Characterization and quantification of microplastics in indoor environments (May). Heliyon 9 (5). https://doi.org/10.1016/J.HELIYON.2023.E15901.
Zhang, Y., et al., 2025. Airborne microplastics (AMPs) and their impact on human health: a critical review (Jun). J. Environ. Sci.. https://doi.org/10.1016/J.JES.2025.06.047.
Zhang, Y., Kang, S., Allen, S., Allen, D., Gao, T., Sillanpää, M., 2020. Atmospheric microplastics: a review on current status and perspectives (Apr). Earth Sci. Rev. 203, 103118. https://doi.org/10.1016/J.EARSCIREV.2020.103118.
Zhu, Y., et al., 2024. A comprehensive review on the source, ingestion route, attachment and toxicity of microplastics/nanoplastics in human systems. J. Environ. Manag. 352, 120039. https://doi.org/10.1016/j.jenvman.2024.120039.
C. Zipeng *et al.*, "Mapping the hidden journey of microplastics: Multi-organ deposition patterns and organ-specific health risks revealed by AI-driven analysis," 2025.